Fabrication of a glycation induced amyloid nanofibril and polyalizarin yellow R nanobiocomposite: Application for electrocatalytic determination of hydrogen peroxide

Nader Amini, Mohammad Bagher Gholivand, Mojtaba Shamsipur, Ali Akbar Moosavi Movahedi, Sara Farahi, Mehran Habibi-Rezaei, Afshin Maleki, Reza Rezaee, Kazhal Naderi

PII: S0141-8130(18)33402-0
DOI: doi:10.1016/j.ijbiomac.2018.10.043
Reference: BIOMAC 10694

To appear in: *International Journal of Biological Macromolecules*

Received date: 5 July 2018
Revised date: 25 September 2018
Accepted date: 10 October 2018

Please cite this article as: Nader Amini, Mohammad Bagher Gholivand, Mojtaba Shamsipur, Ali Akbar Moosavi Movahedi, Sara Farahi, Mehran Habibi-Rezaei, Afshin Maleki, Reza Rezaee, Kazhal Naderi , Fabrication of a glycation induced amyloid nanofibril and polyalizarin yellow R nanobiocomposite: Application for electrocatalytic determination of hydrogen peroxide. Biomac (2018), doi:10.1016/j.ijbiomac.2018.10.043

Fabrication of a glycation induced amyloid nanofibril and polyalizarin yellow R nanobiocomposite: Application for electrocatalytic determination of hydrogen peroxide

Nader Amini[a]*, Mohammad Bagher Gholivand[b], Mojtaba Shamsipur[b]**, Ali Akbar Moosavi Movahedi[d],Sara Farahi [c], Mehran Habibi-Rezaei[c] , Afshin Maleki[a], Reza Rezaee[a], Kazhal Naderi[e]

[a]*Environmental Health Research Center, Research Institute for Health Development, Kurdistan University of Medical Sciences, Sanandaj, Kurdistan, Iran*
[b]*Department of Analytical Chemistry, Razi University, Kermanshah, Iran*
[c] *School of Biology,College of Science,University of Tehran, Iran*
[d]*Institutes of Biochemistry and Biophysics,University of Tehran, Iran*
[e]*Vice chancellor for Food and Drug, Kurdistan University of Medical Sciences, Sanandaj, Kurdistan, Iran*

Abstract

Amyloid fibrils were produced in a solution of bovine serum albumin (BSA) in buffer solution in the presence of fructose. The solution was incubated for 20 weeks in the dark. We used glycation induced bovine serum albumin in which fibrilogenesis (nano fibrils) followed by using fluorescence (Thioflavin T), Dynamic Light Scattering (DLS) and Transmission Electron Microscopy (TEM) to achieve the size and morphology of fibrils. A novel electrochemical biosensor for the detection of hydrogen peroxide was developed based on immobilizing poly (alizarin yellow R) and amyloid nano-fibrils on glassy carbon electrode (PAYR/AMLNFibs/GCE). The electrocatalytic response of the biosensor was proportional to the hydrogen peroxide concentration in the range of 1 µM to 2.2 mM with a limit of detection and sensitivity of 290 nM and 0.024 µA/µM, respectively. The modified electrode demonstrated many advantages such as high sensitivity, low detection of limit and excellent catalytic activity.

Keywords: Amyloid nanofibrils; Glycation; Alizarin yellow R; Hydrogen peroxide; Electrochemical biosensor

.....

*Corresponding authors: Email address: naderamini95@yahoo.com, mshamsipur@yahoo.com, Tel: +98 9183761209

1. Introduction

Glycation occurs through the Maillard reaction in which a reducing sugar reacts with an NH_2 on a protein either at the amino group terminus or at the ε-amino group of lysine remainders. This results in the formation of Amadori products for reaction with glucose or Heyns products for reaction with fructose. These adducts can then further react and rearrange to give a spectrum of products known as advanced glycation end products or AGEs [1]. Organizing capable bio-structures can be achieved by molecular self-assembly [2]. Both in vitro and in vivo amyloid fibrils as filamentous ordered assemblies are formed by many proteins when subjected to glycation [3-5] . Amyloid fibrils offer an energetically stable alternative state for the functionally folded monomeric state of many polypeptides and proteins. The proteins and peptides that form amyloids undergo a structural transition from native soluble monomeric conformations, in many cases via a natively unfolded intermediate, into aggregative fibrillary assemblies that have a predominantly β-sheet structure. Basically, amyloid fibers are a bundle of highly ordered filaments composed of a stepladder of β strands that run perpendicular to the fiber axis and are arranged in hydrogen-bonded β sheets (Figure 1A).

(Figure 1)

Usually, amyloid fibers have a length of up to a few micrometers and a diameter of approximately 7–10 nm. In cross sections, amyloid assemblies appear as ribbons or hollow cylinders. The physical measurements of amyloid fibers illustrated that they are comparable to silk in mechanical stiffness and comparable to steel in strength [6]. The molecular self-assembly of proteins can be accomplished at nano-scale order to provide a three dimensional structure. Amyloid fibrils can be used as nano-scaffolds and support biological agents such as enzymes [7] for nanotechnology applications including roles in catalysis, electronics, plastic, supporting cells and might even be used in therapies [8].

Amyloid fibrils are thermally stable at high temperatures and different pHs. The long and thin fibrils have a high surface-to-volume (and a high aspect) ratio, have usage as carrier systems and contain multiple potential ion-binding sites within the amino acid

sequences [9-13]. Thus, amyloid fibrils have been successfully explored for a number of potential applications such as biosensing, solid functional organic films, hydrogels, fibrous cell scaffolds, nanowire production and bioremediation [14-16].

Hydrogen peroxide (HP) has been used for paper bleaching and the synthesis of various organic compounds as well as an antibacterial agent for many years. HP was used by hospitals and dentists in sterilizing and cleaning. Biological organisms are directly affected by H_2O_2 possibly leading to central nervous system diseases. Therefore, the development of accurate and reliable methods for determination of HP is assumed to be practically important. Several analytical methods such as chromatographic, phosphorescence, fluorescence, spectrophotometric and titrimetric analysis have been developed for the detection and determination of hydrogen peroxide. Although these techniques clearly determine hydrogen peroxide, electrochemical methods have emerged as preferable due to their simple, low cost, high sensitivity and low detection limit.

The electrooxidation or electroreduction of hydrogen peroxide is not appropriate using bare electrodes. Bare electrodes show slow electrode kinetics and high over potential required for these reactions. To overcome this problem, modified electrodes have been extensively used [17]. Many electron transfer mediators, were used for the fabrication of amperometric sensors and biosensors to facilitate voltammetric and amperometric determination and detection. There are many kinds of materials that can be used as electron transfer mediators for the electrocatalytic reduction of H_2O_2 such as Prussian blue and its analogs, polyoxometalates, nano-Au, carbon nano-tube (CNT) and Peroxidases often used by conjugating with nano-ZrO_2, TiO_2, CNT, polymers, non-ionic surfactant triton X-100, nano-Au and sol–gel. However, some of these methods have the complication of electrode fabrication and the disadvantage of slow electron transfer process.

Organic dyes such as methylene blue (MB), meldola blue and methylene green have attracted great attention because of their low-price, fast response and high electrocatalytic activity towards the electrochemical detection of HP [18].

Some of the polymers such as conducting polymers have acquired considerable attention in recent years and deemed to be an important support material for electrochemical sensors and biosensors owing to their strong adherence to electrode surface, reproducibility, good stability and homogeneity in electrochemical deposition

[19]. Electropolymerization is a good method for fabricating modified electrodes by polymer via regulating the electrochemical parameters to adjust film thickness and charge transport characteristics. Organic dyes as specific conducting polymer with a high application potential have become appealing. Many organic dyes including neutral red [20-22], toluidine blue [23], alizarin red S [24], congo red [25-26], nile blue A [27], thionine [28-29] and pyrocatechol violet [30-31] have been successfully used in preparation of electrochemical biosensors and sensors. For instance, Fang et al. [30] presented an H_2O_2 sensor using MWCNTs/poly (pyrocatechol violet) modified electrode; Jeykumari et al. [29] reported an HP sensor based on a thionine functionalized MWCNTs modified electrode; Sheng et al. [31] reported HP determination using pyrocatechol violet modified carbon ceramic electrodes.

Alizarin yellow R is an organic dye occasionally used as a pH indicator [32] and metallochromic indicator [33]. To the best of our knowledge, the usage of amyloide fibrils as a modifier for the fabrication of electrochemical biosensors have never been reported. In our research, by combining the benefits of polyalizarin yellow R (as a conductive polymer) and amyloide nanofibril (having high surface to volume), the resulted PAYR/AMLNFibs/GCE exhibited excellent electrocatalytic activity for the reduction of HP. The proposed method presented a number of attractive features for HP determination including simplicity, low detection limit, stability, high sensitivity and more importantly this biosensor is the first Amyloid fibrils electrode for low level HP monitoring.

2. Experimental

2.1. Reagents

Fructose, Alizarin yellow R and hydrogen peroxide were obtained from Aldrich and Merck and used as received. Buffer solutions (0.1 M) were prepared from di- sodium hydrogen phosphate (Na_2HPO_4), sodium dihydrogen phosphate (NaH_2PO_4), Hydrogen chloride (HCl) and sodium hydroxide (NaOH) acquired from Merck. Bovine serum albumin (BSA) Fraction V, > 95% protein, Congo red, Thioflavin T (ThT) and Uranyl acetate were obtained from, Fluka and PELCO, respectively. Double distillated water was used to prepare all solutions. Other chemicals with analytical grade were purchased from Sigma or Merck and used without further purification. The bleaching cream as the real samples was acquired from a pharmacy.

2.2. Apparatus

Electrochemical experiments were performed with a computer controlled µ-Autolab modular electrochemical system (Eco Chemie U/techt, the Netherlands) driven with GPES software (Eco Chemie). A conventional three-electrode cell consisting of a Ag/AgCl [KCl (sat)], Pt wire and (unmodified or modified) glassy carbon were used as reference, counter and working electrode, respectively. Transmission electron micrographs were recorded on a ZEISS electron microscope (EM 902A) operating at 70 kV at 22000 ×magnification. A Zetasizer Nano S (Malvern) instrument (5 mW HeNe laser, λ=632 nm) was used for assessment of the fibril hydrodynamic diameter (*dh*). The protein fibrillation assessment was achieved by both intrinsic and extrinsic fluorescence strategies using Carry Eclipse spectrofluorometer with the band slit adjusted to 5 nm. A personal computer was used for data analysis.

2.3. Fibril preparation

Amyloid fibrils were produced in a solution of 0.75 mM BSA in PBS (pH 7.4) in the presence of 500 mM fructose. The solution was incubated at 40 ºC for 20 weeks in the dark. The BSA solution was used without any carbohydrate as a control [34]. Figure 2 shows browning through Bovine serum albumin glycation over 20 weeks of incubation. All the bottles are clear from time zero to week 20th. The control group (BSA without fructose) demonstrated no color changes over the 20 weeks of incubation. After 10 weeks, the amyloid precipitates were observed at the bottom of the bottles.

Figure 2

2.4. Preparation of the modified electrode

Before modifying the glassy carbon electrode surface, the bare GCE was carefully polished successively with No. 1 to No. 6 emery papers and 0.5 µm alumina powder. Then, it was sonicated in distilled water and ethanol for 300 seconds to remove adsorbed particles. This was followed by adding 50 µL amyloid nano fibril solution to 3 mL buffer solution and ultra-sonicating it for 3 min to form a homogeneous amyloid

nano fibril solution. Next, 2 µL of this solution was placed on the electrode surface and dried at laboratory temperature.

2.4.1. *Electropolymerization of the alizarin yellow R on* AMLNFibs / GCE

The electropolymerization of alizarin yellow R was performed in the presence of alizarin yellow R in phosphate buffer at the range of potential -1.0 to 1.2 V on AMLNFibs/GCE at pH 11. As Figure1B illustrates, a reduction peak and two oxidation peaks were observed.

Furthermore, with continuous scanning, the oxidation and reduction peak currents were increased. This demonstrates that the continuous growth of the poly (alizarin yellow R) was successfully deposited on the AMLNFibs/GCE. When the cyclic scan was scanned up to 12 cycles, the oxidation and reduction peak currents hardly grew which indicated that polymerization did not occur. Thus, the cyclic scan of 12 was selected to fabricate the PAYR/AMLNFibs/GCE.

3. Results and discussion

3.1. Characterization of Nano-fibril

3.1.1. Fluorescence analysis

Glycation induced fibrillation of BSA was used to provide fibrilar nano-scaffold needed for the immobilization process. The extent of fibrillation was confirmed using various methods. In the presence of fructose, a single molecule of BSA is spontaneously and non-enzymatically glycated and rearranges to form the soluble/toxic pre-fibrils. These pre-fibrils ultimately form the non-soluble/non-toxic fibrils [35-36]. In a ‘‘bottom-up’’ strategy, glycation products aggregate orderly to form complex supra-molecular assemblies which precipitate in the form of non-soluble fibrils in a time dependent manner [34,37]. At the early stage of glycation, the carbonyl groups from reducing sugar side groups and mostly lysine ε-amino groups from protein-side chains react to form Schiff bases which rearrange to form Amadori products. These oxidized and reorganized product species are referred to as AGEs [38]. The formation of the AGE species as the function of time (weeks) is routinely confirmed by the development of β-structures using Congo red binding, and intrinsic fluorescence (λex/em= 450/490 nm) [39- 40]. As expected, a linear increase was observed up to 16 weeks of incubation [34, 37]. The results of benzothiazole dye and thioflavin T (ThT)-based extrinsic

fluorescence assay as the primary method of quantifying amyloid nano-fibril formation [33 35] is shown in Figure 3A. These binding assays further confirmed the development of a nano-fibril.

Furthermore, Congo red (CR) is a commonly used amyloid dye. There is currently no experimentally available structure of CR bound to an amyloid fibril and the binding manners are poorly understood. Both red shift and increasing absorbance at 530 nm in the presence of Congo red can confirm amyloid formation. In this experiment Congo red was used to approved amyloid formation over 20 weeks. The test was carried out every 5 weeks. Red shift and increasing absorbance was significantly observed during incubation time (Figure 3B).

(Figure 3)

3.1.2. Transmission Electron Microscopy (TEM)

Glycated bovine serum albumin was placed on 300-mesh grids. After 1 minute, the buffer was wicked out using filter papers followed by staining samples with uranyl acetate (1%) [7]. TEM images of aggregates revealed aggregation stages from short to long fibrils and from long fibrils to light-scattering fibrils after 20 weeks of incubation (Figure 3C).

3.1.3. Dynamic Light Scattering (DLS)

hydrodynamic diameter (dh). The glycated BSA (0.5 $mg.ml^{-1}$) was taken in a low volume disposable cuvette (1.5 ml volume, path length 1 cm) [1, 7,8]. The hydrodynamic diameter of the mature nano-fibrils at week 20 of incubation was determined using dynamic light scattering (DLS) at the detection angle of 632 nm relative to the incident beam. The DLS image of amyloid fibers with an average size of 10 nm can be seen in Figure 3D.

3.2. Electrochemical characterization of PAYR/AMLNFibs/GCE

For the electrochemical characterization of different electrodes, electrochemical impedance spectroscopy (EIS) was used. Figure 4A shows the impedance spectra represented as Nyquist plots (Zim vs. Zre) for bare GCE (Fig.4A-a), AMLNFibs/GCE (Fig.4A-b), PAYR/AMLNFibs/GCE (Fig.4A-c) and PAYR /GCE (Fig.4A-d) composite film modified electrode in 5 mM $Fe(CN)_6^{3-/4-}$ at 0.22 V and in the frequency range of 0.01 to 10^4 Hz.

In the EIS curves, the semicircle portion regarding electron transfer limited process and its diameter is equal to the electron transfer Rct which controls electron transfer kinetics of redox probe at the electron interface. The EIS data of the three electrodes were fitted on a simple equal circuit shown in the Scheme (Figure 4A - Inset).

In the EIS methods, Rct, C and Rs demonstrate charge transfer resistance, double layer capacitance and the solution resistance, respectively.

(Figure 4)

As observed in the Nyquist plots (Fig.4A), the semicircle of bare electrode (Rct = 5.53 KΩ curve 4A- a) showed the diffusion limiting step of the electrochemical process increase for AMLNFibs/GC (Rct = 8.5 KΩ curve 4B-b) and dramatically decrease for PAYR/ GCE (Rct= 0.0766 KΩ curve 4A-d). When the PAYR/AMLNFibs nanocomposite was immobilized onto the surface of the electrode (Rct = 4.1 KΩ curve 4A-c), the EIS curve diameter became smaller than that of the AMLNFibs and bare GC electrodes. These findings suggest that electron transfer in the PAYR/AMLNFibs /GCE is easier between the surface of electrode and the solution and PAYR/AMLNFibs raises electron transfer confirming the formation of a new layer on the surface of the glassy carbon electrode.

3.3. Electrocatalytic oxidation of hydrogen peroxide on PAYR/AMLNFibs /GCE

In order to investigate electrocatalytic activity, PAYR/AMLNFibs modified GC electrode cyclic voltammetry was used. For comparison, the cyclic voltammograms of unmodified and modified electrodes in the absence and presence of 2.3 mM HP in a 0.1 M buffer solution of pH 6 is illustrated in Figure 4B. For bare GCE in the absence (4B-a) and the presence (4B-b) of HP, no observable reduction current of HP was observed.

For PAYR /GCE (4B-d), a very low reduction current was observed for the electroreduction of HP. For the electrode modified with AMLNFibs (4B-c), a reduction peak was not observed. Remarkably, at the PAYR/AMLNFibs/GCE (4B-e), a higher reduction current of HP was shown.

A notable negative shift of the cathodic peak potential and dramatic increment of current indicated excellent electrocatalytic capability of PAYR/AMLNFibs for HP reduction.

In order to optimize the conditions of the hydrogen peroxide electroreduction at the surface of modified electrodes, the effects of pH solution on the catalytic reduction of hydrogen peroxide on the surface of the modified electrode were studied. The CVs of a 500 µM solution of hydrogen peroxide at different pH values (from 4 to 8) at the PAYR/AMLNFibs modified GC electrode was recorded (not shown).

Since a high electrocatalytic peak current was observed at pH= 6, the hydrogen peroxide analysis was carried out at physiological pH 6 in this research. For evaluating the electrocatalytic activity of PAYR/AMLNFibs, the cyclic voltammograms of the modified electrode in the presence of different concentrations of H_2O_2 (from 50 to 2100 µM) were examined at scan rate of 30 mV/s (Fig.5A). As observed, the HP reduction peak current increased by increasing HP concentration in the buffer solution.

This resulted in a linear curve (inset of Figure 5A) of catodic peak current *vs* hydrogen peroxide concentration with a regression equation of I (µA) = -0.0009 [hydrogen peroxide] µA μM^{-1} – 3.2512 µA, R^2= 0.9823.

Based on the findings, it can be inferred that the detection of hydrogen peroxide at low concentration was facilitated due to the presence of the immobilized PAYR/AMLNFibs nanocomposite at the surface of GC electrode.

(Figure 5)

Figure 5B shows the cyclic voltammograms of 500 µM hydrogen peroxide in a buffer solution of pH 6 at different scan rates. The inset of Figure 5B illustrates that the catodic peak current for reduction of hydrogen peroxide is proportional to square root of the scan rate ($v^{1/2}$) showing that the process is controlled by diffusion as expected for a catalytic system.

3.4. Amperometric detection of hydrogen peroxide *at PAYR/AMLNFibs /GCE*

The amperometry method along with stirred condition is much more current sensitive than cyclic voltammetry. Thus, this method was used in order to assess the low detection limit. The electrocatalytic reduction of hydrogen peroxide by poly PAYR/AMLNFibs modified GC electrode was implemented amperometrically for rotating modified electrode using an applied potential of -0.45 V.

Figure 6 A and B show the typical steady-state catalytic current time response of the rotated modified electrode (2000 rpm) with successive injection of hydrogen peroxide at an applied potential of -0.45 V vs. Ag/AgCl reference electrode.

The results show that a good defined response was obtained during the consecutive addition of 150 µM of hydrogen peroxide. The findings also demonstrate the efficient catalytic property of the PAYR/AMLNFibs immobilized on the surface of GC electrode. As revealed, there is a linear relation between current and hydrogen peroxide concentrations in the range of 1 µM – 2.2 mM (Figures 6 a and b), while for a higher concentration of hydrogen peroxide, the plot of current vs. HP concentration deviates from linearity. The linear least squares calibration curve over the range 1–20 µM (20 points) is I (µA) = 0.0198 [hydrogen peroxide] + 0.0935 µA with a correlation coefficient of 0.9849 indicating that the regression line is very well fitted with the experimental data. In addition, the regression equation can be used for determination of unknown samples. The detection limit (signal to noise of 3) and sensitivity were 290 nM and 0.024 µA/µM, respectively [44].

(Figure 6)

3.5. Comparison of the proposed biosensor with those of previous electrochemical methods

Table 1 compares the limit of detection, linear range and sensitivity of the proposed biosensor for hydrogen peroxide determination with those of other hydrogen peroxide electrodes previously reported [45-53]. As can be seen from this table, the detection limit of the proposed electrode is lower than all of the electrodes mentioned in this table except for items 48 and 53. Moreover, the linear range is better than that of items 46,

47, 50 and 52 and the sensitivity parameter calculated was better or comparable with that of other electrodes.

(Table 1)

3.6. Determination of H_2O_2 in real samples

To use the proposed biosensor, the determination of H_2O_2 at various milk samples using cyclic voltammetric method was evaluated. The concentration of H_2O_2 in the two different milk samples purchased from the market were investigated. The samples were spiked with 50 μM and 70 μM of H_2O_2 and the recovery of H_2O_2 was calculated. The hydrogen peroxide concentration determined in samples using our proposed electrode is listed (Table 2). First, a blank milk sample was evaluated in the same way but did not show any current response. The RSD and excellent recoveries reported in Table 2 clearly indicated the reliability of the proposed biosensor for determination of HP in milk samples

(Table 2)

3.7. Repeatability and lifetime

The lifetime and repeatability of the PAYR/AMLNFibs /GCE were calculated at H_2O_2 concentration of 50 μM. The R.S.D obtained was 5% for five successive assays. The stability and lifetime of the biosensor were estimated by measuring the response current of the biosensor after one week and one month and the observed decreases in the electrode response were 96.1% and 91.5% of initial current, respectively.

4. Conclusion

In conclusion, we introduced a novel modified electrode based on immobilizing of amyloid nanofibriles onto electrode surface. The glycation reaction and the electropolymerization method were used for preparation of amyloid nanofibril and polyalizarine, respectivly. The TEM and DLS measurements revealed the formation of amyloid nanofibriles. The PAYR/AMLNFibs /GCE showed efficient catalytic activity in the electrochemical reduction of hydrogen peroxide. The best reduction peak current was observed at neutral pH. As observed in Table 1, the proposed electrode has greater advantages than that reported in this Table. This method could be extended to other nanofibrils and has potential usage in the design of electrochemical biosensors for other samples.

Legends to the Figures:

Figure 1. (A) The formation of amyloid fibrils. Anatively folded monomer undergoes a conformational transition into a β--sheet-rich state, usually through a partial unfolded state. Self-assembly of these intermediates into ladders of β- strands results in the formation of ordered filaments that aggregate into the well-known amyloid fibrils.
(B) The continuous CVs for the electropolymerization of alizarin yellow R on GCE in 0.1 M phosphate buffered (pH11) at 100 mVs^{-1}.

Figure 2. Bovine serum albumin glycation over 20 weeks of incubation.

Figure 3. (A) Fluorescence spectra of (a) nonglycated and (b) glycated albumins; (B) Congo Red absorbance spectra during incubation time; (C) TEM image of nanofibrils; (D) The Dynamic light scattering of nano-fibrils.

Figure 4. (A) Electrochemical impedance spectroscopy (EIS) of bare GCE (Figure 3A-a), AMLNFibs/GCE (Figure 3A-b), PAYR/AMLNFibs/GCE (Figure 3A-c) and PAYR /GCE (Figure 3A-d) in 5 mM probe $Fe(CN)_6^{4-/3-}$.
(B) Cyclic voltammetry response of unmodified electrode in the absence (a) and presence (b) of hydrogen peroxide, and (c) AMLNFibs (d)PAYR(e)PAYR/AMLNFibs modified GC electrode in the presence 50 µM of hydrogen peroxide at scan rate of 30 mVs^{-1}, pH= 6.

Figure 5. (A) Cyclic voltammogram of PAYR/AMLNFibs modified GC electrode in pH = 6 buffer containing different concentration of hydrogen peroxide from 50,200,300,400,500,600,800,1000,1200,1400,1600,1800 and 2100 µM. Inset shows plot of peak current vs, hydrogen peroxide concentration at scan rate of 30 mVs^{-1}
(B) Cyclic voltammetry response of a GCE modified with PAYR/AMLNFibs modified GC in a phosphate buffer (pH 6) containing 500 µM of hydrogen peroxide at different scan rates of (from inner to outer) 10-100 mVs^{-1}. Inset illustrates plot of peak current vs, $v^{1/2}$.

Figure 6. Amperometric response at rotating poly PAYR/AMLNFibs modified GC electrode (rotation speed of 2000 rpm) held at -0.45 V in buffer solution (pH6) for successive addition of (A) 150 µM hydrogen peroxide and (B) 1 µM hydrogen peroxide (a and b). Plot of amperometric currents vs. hydrogen peroxide concentrations.

Table 1. Analytical parameters of several modified electrodes for determination of hydrogen peroxide.

Table 2. Determination of H_2O_2 in milk

References

[1] J. F. Povey, M. J. Howard, R. A. Williamson, C. M. Smales.The effect of peptide glycation on local secondary structure Journal of Structural Biology. 161 (2008) 151–161

[2] K. Rajagopal, J.P. Schneider,Self-assembeling peptides and proteins for nanotechnologycal application. Curr. Opin. Struct. Biol. 14 (2004) 480–486.

[3] N. Sattarahmady, A.A. Moosavi-Movahedi, M. Habibi-Rezaei, S. Ahmadian, A.A. Saboury, H. Heli, N. Sheibani, Detergency effect of nanofibrillar amyloid formation on glycation of huma serum albumin Carbohydr. Res. 343 (2008) 2229–2234.

[4] A.L. Fink, Protein aggregation: folding aggregate, inclusion bodies and amyloid Fold. Des. 3 (1998) 9–23.

[5] V.A. Hughes, D.E. Dunstan, Modern Biopolymer Science: Bridging the Divide between Fundamental Treatise and Industrial Application, In: Stephan Kasapis, Ian T. Norton, Johan B. Ubbink (Eds.), Amyloid Fibrils – Self-Assembling Proteins, Academic press, London, 2009, pp. 559–589.

[6] I. Cherny , E. Gazit,Amyloids: Not Only Pathological Agents but Also Ordered Nanomaterials Angew. Chem. Int. Ed. 47 (2008) 4062 – 4069.

[7] E. Gazit, Self-assembled peptide nanostructures: the design of molecular building blocks and their technological utilization,Chem. Soc. Rev. 36 (2006) 1263–1269.

[8] Victoria A. Hughes and Dave E. Dunstan Amyloid Fibrils – Self-Assembling ProteinsKasapis, Norton, and Ubbink: Modern Biopolymer Science _ 2009 Elsevier Inc. ISBN: 978-0-12-374195-0 All rights Reserved CHAPTER 17-P559-594.

[9] S. Bolisetty, M. Arcari, J. Adamcik, R. Mezzenga, Hybrid Amyloid Membranes for Continuous Flow Catalysis, Langmuir 31 (2015) 13867-13873.

[10] J. Han, J. Dai, L. Li, P. Fang, R. Guo, Highly Uniform Self-Assembled Conducting Polymer/Gold Fibrous Nanocomposites: Additive-Free Controllable Synthesis and Application as Efficient Recyclable Catalysts, Langmuir 27 (2011) 2181-2187.

[11] H. Wang, G.L. Rempel, Bimetallic Dendrimer-encapsulated Nanoparticle Catalysts, Polym. Rev. 56 (2016) 486-511.

[12] C. Li, J. Adamcik, R. Mezzenga, Biodegradable nanocomposites of amyloid fibrils and graphene with shape-memory and enzyme-sensing properties. Nat. Nano. 7 (2012) 421-427.

[13] J. Juárez, A. Cambón, A. Topete, P. Taboada, V. Mosquera, OneDimensional Magnetic Nanowires Obtained by Protein Fibril Biotemplating. Chem. -Eur. J. 17 (2011)7366-7373.

[14] T.P.J. Knowles, T.W. Oppenheim, A.K. Buell, D.Y. Chirgadze, M.E. Welland, Nanostructured films from hierarchical self-assembly of amyloidogenic proteins, Nat. Nano. 5 (2010) 204-207

[15] C.A.E. Hauser, S. Maurer-Stroh, I.C. Martins, Amyloid-based nanosensors and nanodevices Chem. Soc. Rev. 43 (2014) 5326-5345.

[16] A.M. Smith, R.J. Williams, C. Tang, P. Coppo, R.F. Collins, M.L. Turner, A. Saiani, R.V. Ulijn, Fmoc- Diphenylalanine Self Assembles to a Hydrogel via a Novel Architecture Based on π–π Interlocked β- Sheets Adv. Mater. 20 (2008)37-41.

[17] S. Thiagarajan, Su, S.Chen, Nano TiO_2–Au–KI film sensor for the electrocatalytic oxidation of hydrogen peroxide. Sensors and Actuators B. 136 (2009) 464–471

[18] Q. Sheng, H. Yu, J. Zheng, Hydrogen peroxide determination by carbon ceramic electrodes modified with pyrocatechol viole, Electrochimica Acta, 52 (2007) 7300–7306.

[19]. K. Doblhofer, Electrodes covered with thin, permeable polymer films, Electrochim Acta, 25 (1980) 871-878.

[20] U. Yogeswaran, S.M. Chen, Separation and concentration effect of f-MWCNTs on electrocatalytic responses of ascorbic acid, dopamine and uric acid at f-MWCNTs incorporated with poly (neutral red) composite films, Electrochim Acta , 52(2007) 5985-5996.

[21] D. R S. Jeykumari, S. S.Narayanan, A novel nanobiocomposite based glucose biosensor using neutral red functionalized carbon nanotubes. Biosens Bioelectron, 23 (2008) 1404-1411.

[22] K.Y. Zhang, Y.Z. Zhang, Lable-free electrochemical DNA sensor based on gold nanoparticles/poly (neutral red) modified electrode, Electroanalysis, 22(2010) 673-679.

[23] J.X. Zeng, W. Z. Wei, L. Wu, X.Y. Liu, K. Liu, Y. Li, Fabrication of poly (toluidine blue O)/carbon nanotube composite nanowires and its stable low-potential detection of NADH, J Electroanal Chem , 595 (2006) 152-160.

[24] K.B. Wu, S.S. Hu, Deposition of a thin film of carbon nanotubes onto a glassy carbon electrode by electropolymerization, Carbon, 42 (2004) 3237-3242.

[25] C.G Hu, X.X. Chen, S.S. Hu, Water-soluble single-walled carbon nanotubes films: preparation, characterization and applications as electrochemical sensing films, Electroanal Chem, 586(2006) 77-85.

[26] C.G. Hu, C.H. Yang, S.S. Hu, and Hydrophobic adsorption of surfactants on water-soluble carbon nanotubes: a simple approach to improve sensitivity and antifouling capacity of carbon nanotubes-based electrochemical sensors, Electrochem Commun, 9 (2007) 128-134.

[27] P. Du, B. Zhou, C.X. Cai, Development of an amperometric biosensor for glucose based on electrocatalytic reduction of hydrogen peroxide at the single-walled carbon nanotube/nile blue A nanocomposite modified electrode, J Electroanal Chem, 614 (2008)149-156.

[28] K.Y. Zhang, L. Zhang, J.G. Xu, C. Wang, T. H.Y.Wang, J. Zhu, A sensitive amperometric hydrogen peroxide sensor based on thionin/EDTA/carbon nanotubes—chitosan composite film modified electrode, Microchim Acta ,171(2010)139-144.

[29] D.R. S. Jeykumari, S. Ramaprabhu, S. S. Narayanan, A thionine functionalized multiwalled carbon nanotube modified electrode for the determination of hydrogen peroxide. Carbon 45 (2007) 1340-1353.

[30] B. Fang, N. Zhang, W. Zhang, A.X. Gu, G.F. Wang, A novel hydrogen peroxide sensor based on multiwalled carbon nanotubes/poly (pyrocatechol violet)-modified glassy carbon electrode, J Appl Polym Sci, 112(2009) 3488-3493.

[31] Q.L. Sheng, H. Yu, J.B. Zheng, Hydrogen peroxide determination by carbon ceramic electrodes modified with pyrocatechol violet, Electrochim Acta, 52 (2007) 7300-7306.

[32] T.R. Williams, M. Lautenschleger, Titration of weak acids with tetramethylgnanidine as solvent, Talanta, 10 (1963) 804-808.

[33] K. Ihara, S.I. Hasegawa, K. Naito, The separation of aluminum (III) ions from the aqueous solution on membrane filter using Alizarin Yellow R, Talanta, 75 (2008) 944-949.

[34] B. Bouma, L.M.J. Kroon-Batenburg, Y.P. Wu, B. Brunjes, G. Posthuma, O. Kranenburg, P.G. de Groot, E.E. Voest, M.F.B.G. Gebbink, Glycation Induces Formation of Amyloid Cross-β Structure in Albumin. J. Biol. Chem, 278 (2003) 41810–41819.

[35] M. Bucciantini, E. Giannoni, F. Chiti, F. Baroni, L. Formigli, J. Zurdo, N. Taddei, G. Ramponi, C. M. Dobson, M. Stefani, Inherent toxicity of aggregates implies a common mechanism for protein misfolding diseases Nat, 416(2002)507-511.

[36] J. Hardy, D. J. Selkoe, The Amyloid Hypothesis of Alzheimer's Disease: Progress and Problems on the Road to Therapeutics,Sci., 297(2002) 353-356.

[37] D.E. Barlow, G.H. Dickinson, B. Orihuela, J.L.Kulp, D. Rittschof, K J. Wahl, Characterization of the Adhesive Plaque of the Barnacle Balanus amphitrite: Amyloid-Like Nanofibrils Are a Major Component, Langmuir , 26(2010) 6549–6556.

[38] P. Rondeau, G. Navarra, Thermal aggregation of glycated bovine serum albumin Biochim.Biophys.Acta., 1804(2010) 789–798.

[39] R.G. Moulick, J. Bhattacharya, Compensatory secondary structure alterations in protein glycation,Biochim. Biophys. Acta., 1774(2007)233–242.

[40] M Nowicki, B Lewczuk, M Papiewska, B Przybylska-Gornowicz, Demonstration of nerve fibers immunoreactive to peptide N-terminal histidine C-terminal isoleucine (PHI) and vasoactive intestinal peptide (VIP) in the pig pineal gland, Folia Histochemica et Cytobiologica 41(2003) 141-147.

[41] M.R. Nilsson, Techniques to study amyloid fibril formation in vitro Methods, 34(2004) 151–160.

[42] S.A. Hudson, H.Ecroyd, T.W. Kee, J.A. Carver, The thioflavin T fluorescence assay for amyloid fibril detection can be biased by the presence of exogenous compounds FEBS , 276(2009)5960–5972.

[43] S.G. Bolder,L.M.Sagis, P. Venema,E. van der Linden, Thioflavin T and Birefringence Assays to Determine the Conversion of Proteins into Fibrils Langmuir, 23(2007)4144–4147.

[44] J.C. Miller, J.N. Miller. Statistics for analytical chemistry 3rd ed. New York : Ellis Horwood PTR Prentice Hall, 1993.

[45] M. Shamsipur, M. Asgari, M.F. Mousavi, R. Davarkhah, A Novel Hydrogen Peroxide Sensor Based on the Direct Electron Transfer of Catalase Immobilized on Nano-Sized NiO/MWCNTs Composite Film Electroanalysis 24 (2012) 357–367.

[46] H. Li,W. Hao, J. Hu,H. Wu, A photoelectrochemical sensor based on nickel hydroxyl-oxide modified n-silicon electrode for hydrogen peroxide detection in an alkaline solution, Biosensors and Bioelectronics, 47 (2013) 225–230

[47] Y. Xia, W.Li, M.Wang, Z.Nie, C.Deng, S.Yao, A sensitive enzymeless sensor for hydrogen peroxide based on the polynucleotide-templated silver nanoclusters/graphene modified electrode, Talanta,107(2013) 55–60

[48] W.Guo, F.Jiang,J.Chu, D.Song, G.Liu, A stable interface based on aryl diazonium salts/SWNTs modified gold electrodes for sensitive detection of hydrogen peroxide, Journal of Electroanalytical Chemistry, 703(2013) 63–69

[49] S.Tian, Q.Zhou, Z.GU, X. Gu, L.Zhao, Y.Li , J.Zheng, Hydrogen peroxide biosensor based on microperoxidase-11 immobilized in a silica cavity array electrode, Talanta, 107(2013), 324–331.

[50] M. Magro, D.Baratella, N.Piance, A.Toninello, S.Grancara,R.Zboril, F.Vianello, Electrochemical determination of hydrogen peroxide production by isolated mitochondria: A novel nanocomposite carbon–maghemite nanoparticle electrode, Sensors and Actuators B: Chemical, 176(2013) 315–322.

[51] C. Priya, G. Sivasankari, S. Sriman Narayanan, Electrochemical behavior of Azure A/gold nanoclusters modified electrode and its application as non-enzymatic hydrogen peroxide sensor, Colloids and Surfaces B: Biointerfaces 97 (2012) 90– 96

[52] A. Salimi, A. Noorbakhsh, M. Ghadermarzi, Direct electrochemistry and electrocatalytic activity of catalase incorporated onto multiwall carbon nanotubes-modified glassy carbon electrode Anal. Biochem. 344 (2005) 16–24.

[53] M.E. Karami, A. Salimi, R. Sahraei, Amperometric detection of hydrogen peroxide at nano-ruthenium oxide/riboflavin nanocomposite-modified glassy carbon electrodes, Electrochimica Acta, 113 (2013) 134–140.

Electrode	LOD (nM)	Sensivity nA/μM	Dynamic linear range	Ref.
GC/MWCNTs/NiO/ Catalase	19×10^{3}nM	337.58μA mM^{-1} cm^{-2}	0.20 to 2.53mM	45
nickel hydroxyl-oxide modified n-silicon	2.2 μM	–	1.0×10^{-5} to 6×10^{-5} M	46
polynucleotide-templated silver nanoclusters/graphene	3 μM	–	15 μM to 23 mM	47
aryl diazonium salts/SWNTs modified gold electrodes	10 nM	–	0.01 to 24 μM	48
microperoxidase-11 immobilized in a silica cavity	4×10^{-7} M	–	2×10^{-6} to 6×10^{-4} M.	49
carbon–maghemite nanoparticle electrode	2.78 μM	58 nA μM^{-1} cm^{-2}	0.01 to1.5 mM	50
Azure A/gold nanoclusters	1.08×10^{-6} M	–	3.26×10^{-6}M to 3.2×10^{-3}M	51
Catalase-MWCNTs	4000 nM	3.3μA mM^{-1} cm^{-2}	0.01 to 0.1mM	52
RuO/Riboflavine/GCE	150 nM	35 nA μM^{-1}	0.15μM to 3mM	53
poly (alizarin yellow R)/nao-fibs/GCE	290 nM	0.024 μA/μM	1 μM to 2.2 mM	This work

Table.1

Sample	H_2O_2 added(μM)	H_2O_2 found (μM)[b]	Recovery (%)
1	50	49. 9 ± (2.4)	99.8
2	70	71.25 ± (2.02)	101.7

[b]Average of two determinations ± relative standard deviation.

Table.2

Highlights

►Amyloid nanofibriles were prepared by reaction between reducing sugars and amino groups of protein for 20 weeks ► For the first time, Amyloid nanofibriles and polyalizarine yellow R were immobolized on to the surface of electrode for fabrication of electrochemical biosensor►The biosensor was used for enhanced electrocatalytic reduction and detection of hydrogen peroxide► The biosensor was applied for analysis of hydrogen peroxide in real samples.

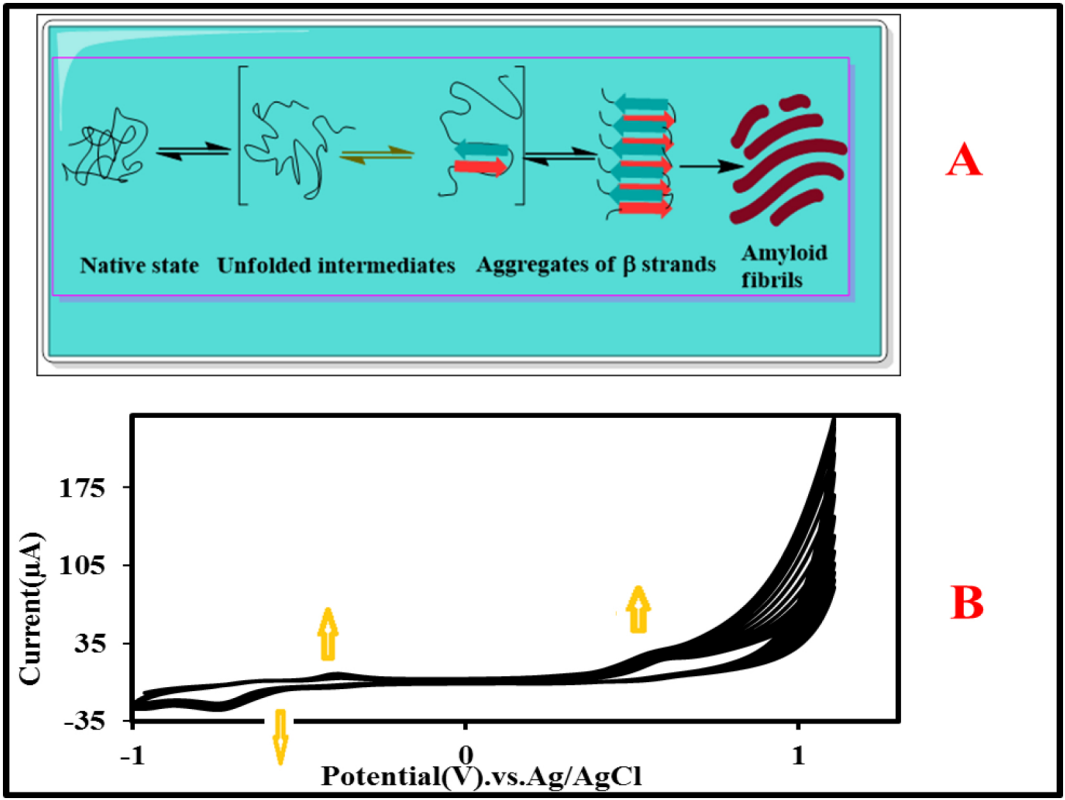
A
Native state
Unfolded intermediates
Aggregates of β strands
Amyloid fibrils
B
175
105
35
-35
Current(μA)
-1
0
1
Potential(V).vs.Ag/AgCl

Figure 1

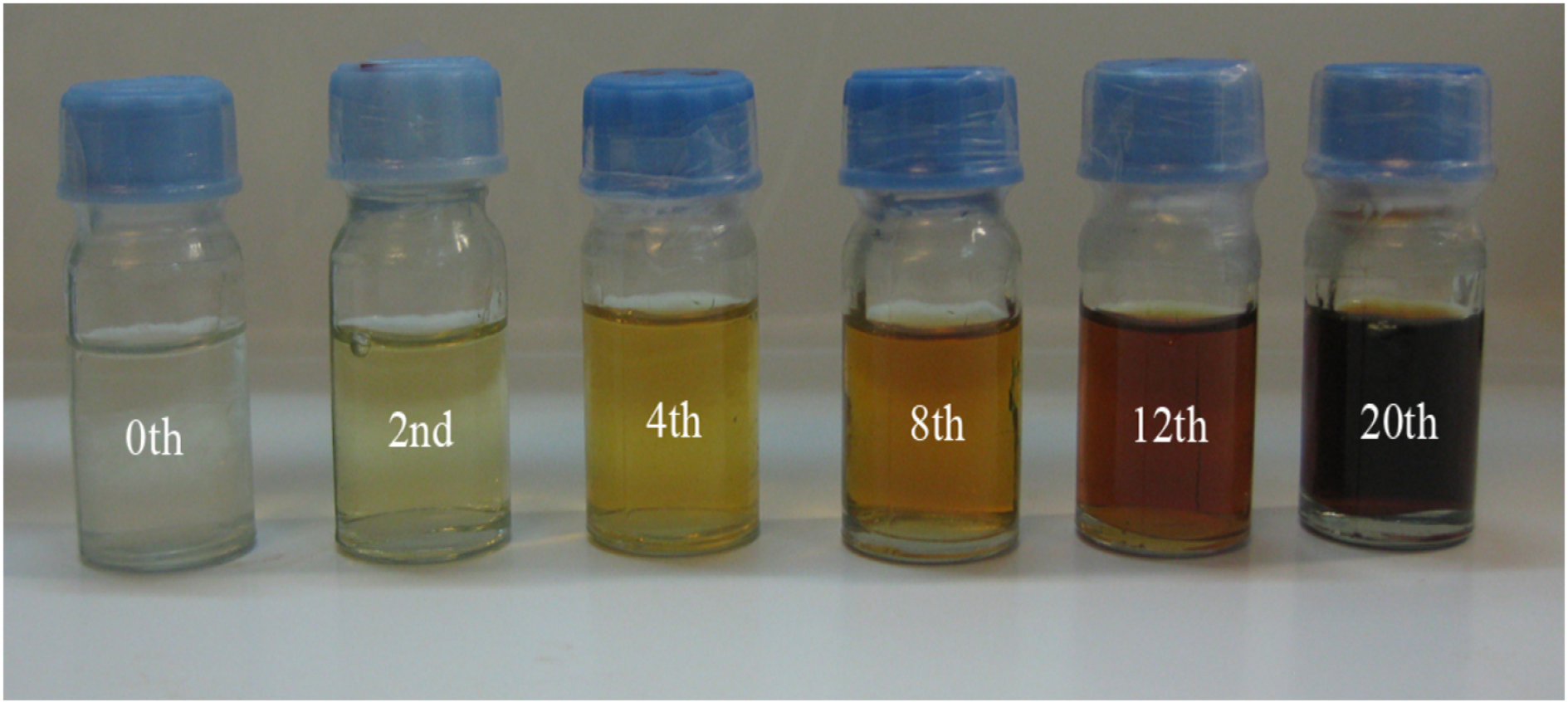

Figure 2

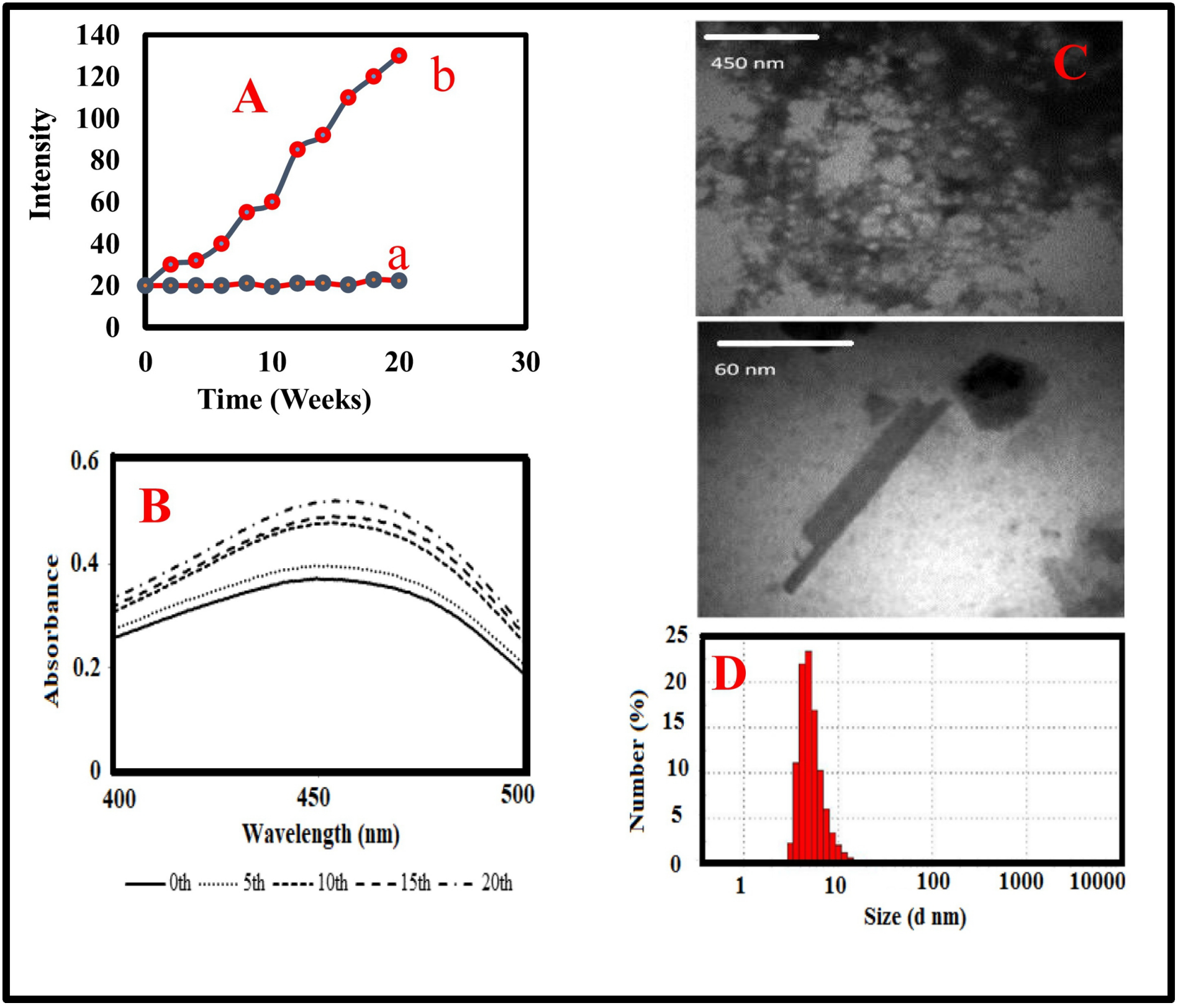
A
b
a
Intensity
Time (Weeks)
B
Absorbance
Wavelength (nm)
0th
5th
10th
15th
20th
C
450 nm
60 nm
D
Number (%)
Size (d nm)

Figure 3

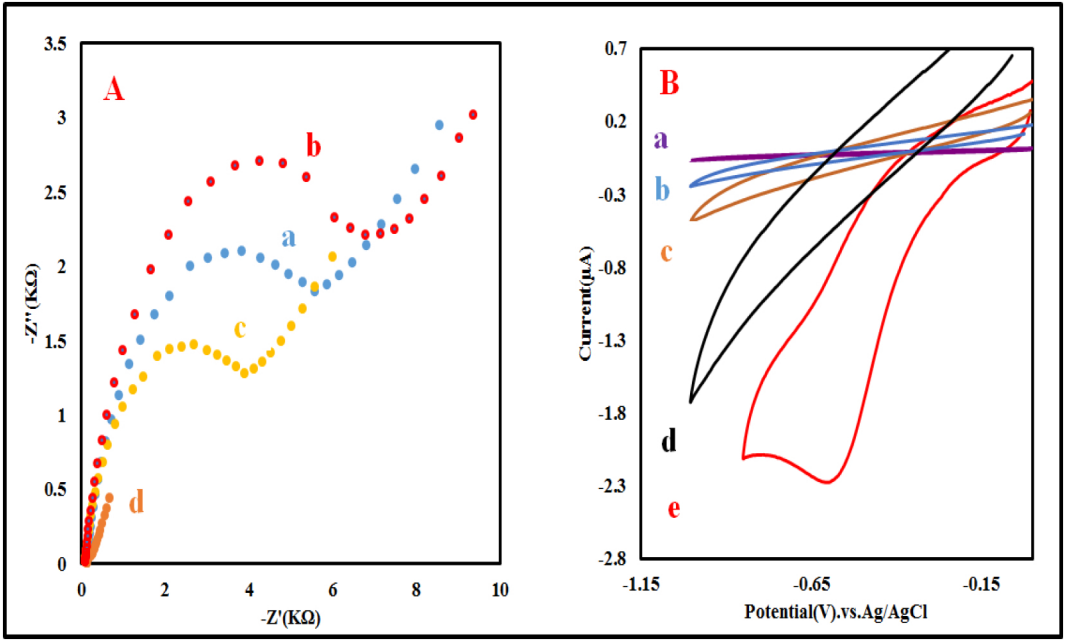
A
b
a
c
d
-Z''(KΩ)
-Z'(KΩ)
3.5
3
2.5
2
1.5
1
0.5
0
0
2
4
6
8
10
B
a
b
c
d
e
Current(μA)
0.7
0.2
-0.3
-0.8
-1.3
-1.8
-2.3
-2.8
-1.15
-0.65
-0.15
Potential(V).vs.Ag/AgCl

Figure 4

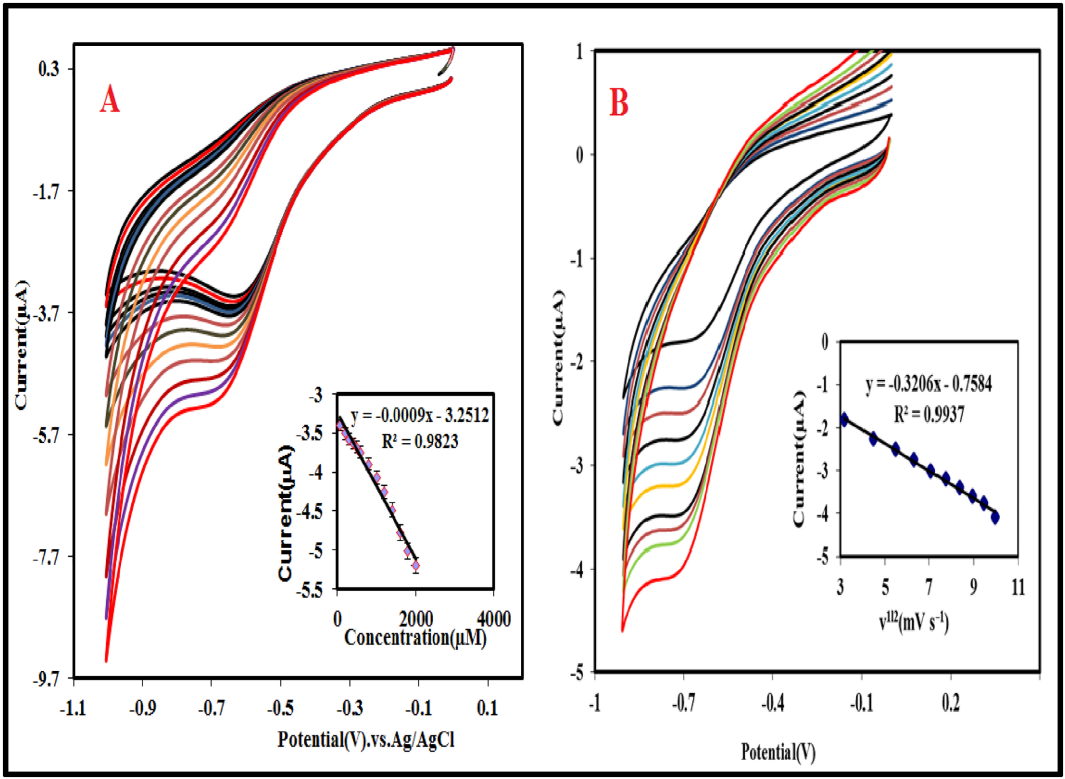
A
Current(μA)
Potential(V).vs.Ag/AgCl
y = -0.0009x - 3.2512
R² = 0.9823
Current(μA)
Concentration(μM)
B
Current(μA)
Potential(V)
y = -0.3206x - 0.7584
R² = 0.9937
Current(μA)
v^1/2(mV s^-1)

Figure 5

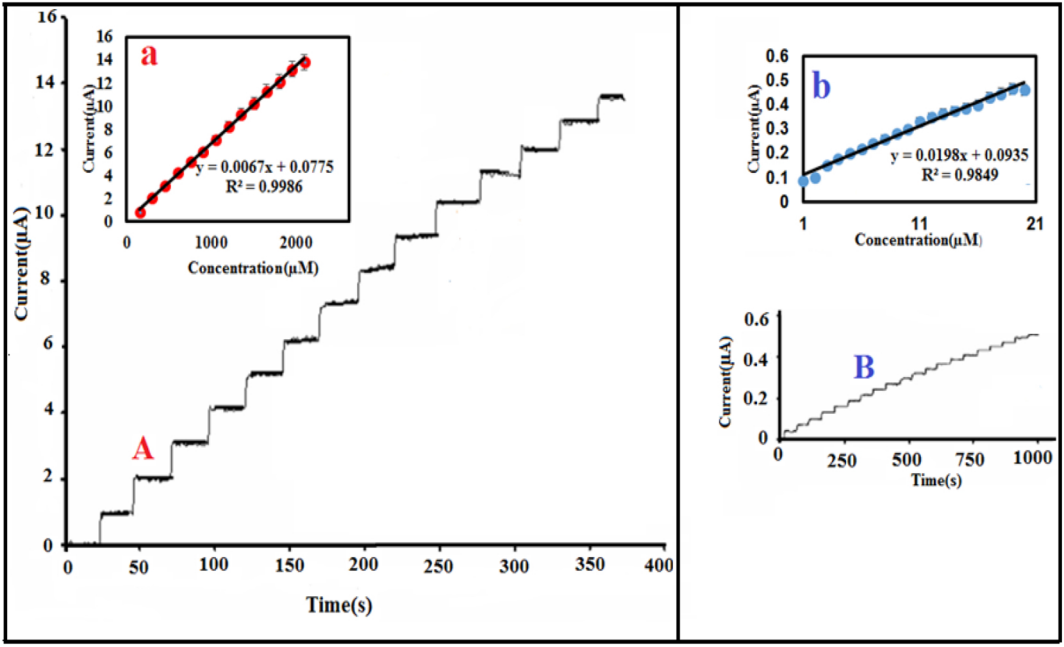
a
Current(μA)
Concentration(μM)
y = 0.0067x + 0.0775
R² = 0.9986
A
Current(μA)
Time(s)
b
Current(μA)
Concentration(μM)
y = 0.0198x + 0.0935
R² = 0.9849
B
Current(μA)
Time(s)

Figure 6